

Neoalbaconol induces energy depletion and multiple cell death in cancer cells by targeting PDK1-PI3-K/Akt signaling pathway

Q Deng^{1,2,3,7}, X Yu^{1,2,3,7}, L Xiao^{1,2,3}, Z Hu^{1,2,3}, X Luo^{1,2,3}, Y Tao^{1,2,3}, L Yang^{1,2,3,4}, X Liu^{1,2,3}, H Chen⁶, Z Ding⁵, T Feng⁵, Y Tang^{1,2,3}, X Weng^{1,2,3}, J Gao^{1,2,3}, W Yi^{1,2,3}, AM Bode⁶, Z Dong⁶, J Liu^{*,5} and Y Cao^{*,1,2,3,4}

Many natural compounds derived from plants or microbes show promising potential for anticancer treatment, but few have been found to target energy-relevant regulators. In this study, we report that neoalbaconol (NA), a novel small-molecular compound isolated from the fungus, *Albatrellus confluens*, could target 3-phosphoinositide-dependent protein kinase 1 (PDK1) and inhibit its downstream phosphoinositide-3 kinase (PI3-K)/Akt-hexokinase 2 (HK2) pathway, which eventually resulted in energy depletion. By targeting PDK1, NA reduced the consumption of glucose and ATP generation, activated autophagy and caused apoptotic and necroptotic death of cancer cells through independent pathway. Necroptosis was remarkably induced, which was confirmed by several necroptosis-specific markers: the activation of autophagy, presence of necrotic morphology, increase of receptor-interacting protein 1 (RIP1)/RIP3 colocalization and interaction and rescued by necroptosis inhibitor necrostatin-1. The possibility that Akt overexpression reversed the NA-induced energy crisis confirmed the importance of the PDK1-Akt-energy pathway in NA-mediated cell death. Moreover, NA shows the capability to inhibit PI3-K/Akt signaling and suppress tumor growth in the nasopharyngeal carcinoma (NPC) nude mouse model. These results supported the feasibility of NA in anticancer treatments.

Cell Death and Disease (2013) 4, e804; doi:10.1038/cddis.2013.324; published online 19 September 2013

Subject Category: Cancer

Over the past several decades, many natural compounds derived from plants or microbes have shown promising potential in cancer chemoprevention and therapy.^{1,2} These natural compounds are almost always with specific structures and unique biologic activities. *Albatrellus confluens*, mainly distributed in southwest China, is a member of the *Polyporaceae* family. Several compounds with anticancer potential have been isolated from this fungus.^{3–5} Recently, neoalbaconol (NA), a novel small-molecular compound with a drimane-type sesquiterpenoid structure (Figure 1a), was isolated from the fruiting body of *Albatrellus confluens*.

The efficacy of tested compounds in the induction of cell death has become the principal standard to assess their feasibility in anticancer treatments, because evasion from cell death has been recognized as one of the most distinguished features of cancer cells;⁶ it is even more meaningful if a compound could induce alternative cell death, as most cancer cells obtain defective cell death apparatus during cancer

development.⁷ Three major forms of cell death have been described, including apoptosis (type I), cell death associated with autophagy (type II) and necrosis (type III).⁸ Traditionally, necrosis has been considered as accidental and unregulated, whereas apoptosis and autophagic cell death have been regarded as 'programmed cell death'.⁸ The classic morphological change of autophagic cells is the abundant autophagic vacuoles present in the cytoplasm. Besides morphological changes, microtubule-associated protein 1 light chain 3 (LC3) has been widely used as an autophagosomal marker to identify autophagy in mammalian cells.^{9,10} Accumulating evidence suggests that in some situations, necrosis is also controlled and programmed in a manner similar to apoptosis; this programmed necrosis is referred to necroptosis.¹¹ Necroptosis is characterized by the activation of autophagy with a necrotic morphology, and this type of cell death can be specifically inhibited by a small compound necrostatin-1 (Nec-1).^{11,12} Under stress conditions, receptor-interacting

¹Xiangya School of Medicine, Cancer Research Institute, Central South University, Hunan, China; ²Key Laboratory of Chinese Ministry of Education, Central South University, Hunan, China; ³Key Laboratory of Carcinogenesis of Chinese Ministry of Public Health, Central South University, Hunan, China; ⁴Molecular Imaging Center, Central South University, Hunan, China; ⁵State Key Laboratory of Phytochemistry and Plant Resources in West China, Kunming Institute of Botany, Chinese Academy of Sciences, Yunnan, China and ⁶The Hormel Institute, University of Minnesota, Austin, Minnesota, USA

*Corresponding authors: J Liu, Kunming Institute of Botany, Chinese Academy of Sciences, 132 no. Heilongtan Lanhei Road, Kunming 650204, Yunnan, China. Tel: +86 0871 6521 2285; Fax: +86 0871 6521 9934; E-mail: jkliu@mail.kib.ac.cn or Y Cao, Xiangya School of Medicine, Cancer Research Institute, Central South University, 110 no. Xiang Ya Road, Changsha 410078, Hunan, China. Tel: +86 0731 8480 5448; Fax: +86 0731 8447 0589; E-mail: ycao98@vip.sina.com

⁷These authors equally contributed to this work.

Keywords: neoalbaconol; PDK1; PI3-K/Akt; energy depletion; cancer cell death

Abbreviations: NA, neoalbaconol; PDK1, 3-phosphoinositide-dependent protein kinase 1; HK2, hexokinase 2; JNKs, c-Jun NH (2)-terminal kinases; NPC, nasopharyngeal carcinoma; LC3, light chain 3; DR, death receptors; Nec-1, necrostatin-1; RIP1, receptor-interacting protein 1; cIAPs, cellular inhibitors of apoptosis; CYLD, cylindromatosis; zVAD-fmk, benzyloxycarbonyl-Val-Ala-Asp(OMe)-fluoromethylketone; 3-MA, 3-methyladenine; Baf, Bafilomycin

Received 13.5.13; revised 26.7.13; accepted 29.7.13; Edited by A Stephanou

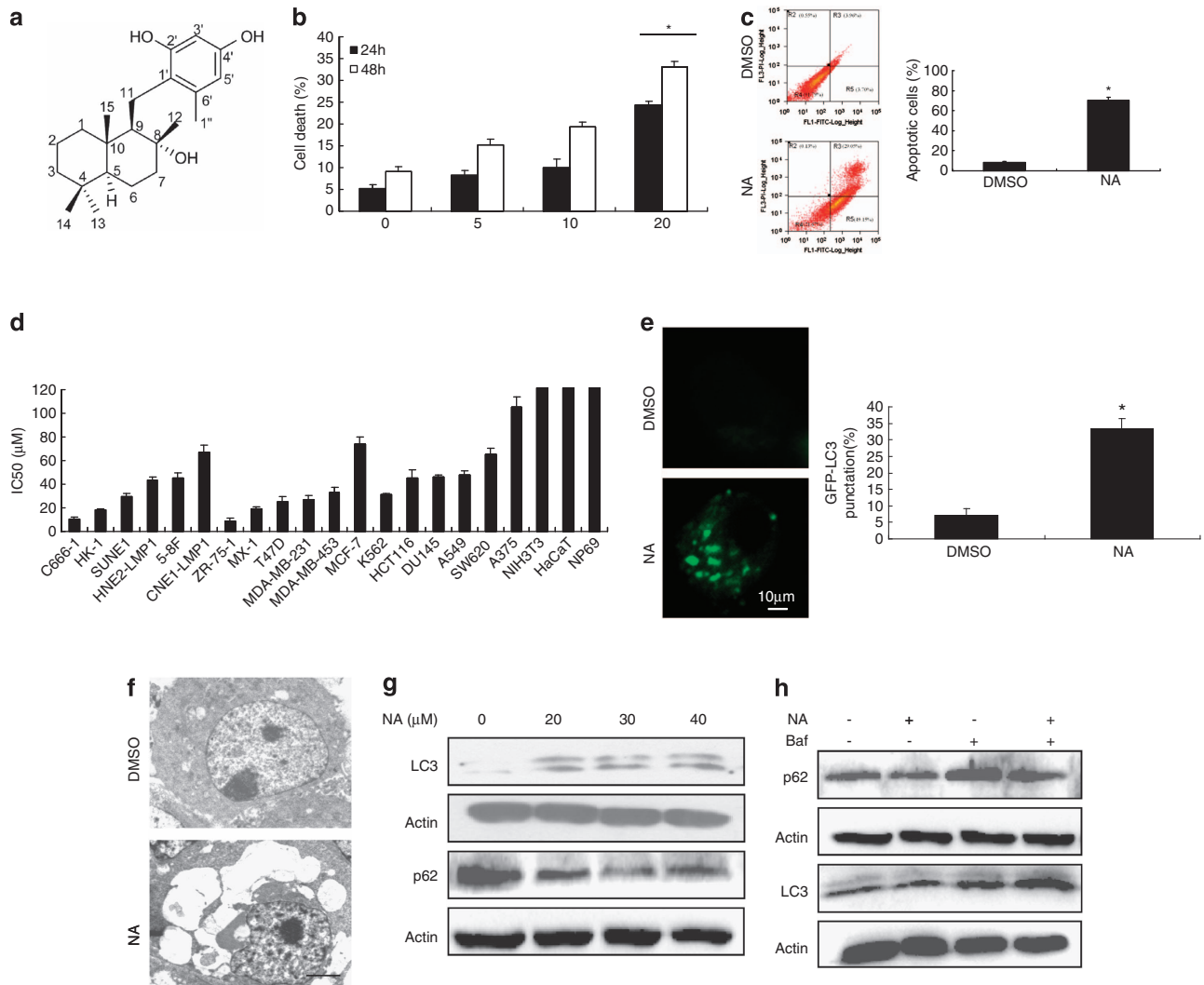


Figure 1 NA selectively inhibits proliferation and induces apoptosis and autophagy in cancer cells. **(a)** The molecular structure of NA. **(b)** The effect of NA in killing C666-1 cells was analyzed using PI staining and flow cytometry analysis. Each histogram is representative of three experiments. Data shown are the mean + S.D. * $P < 0.05$. **(c)** annexin V-FITC/PI double staining and cytometry analysis were adopted to analyze NA-induced apoptosis in C666-1 cells. Each histogram is representative of three experiments. Data shown are the mean + S.D. * $P < 0.05$. **(d)** The effect of NA on cell proliferation was analyzed in different cell lines. IC₅₀ values were calculated with SPSS 16.0 and data shown are the mean + S.D. of three experiments. **(e)** The YFP-LC3 expression plasmid was transfected into C666-1 cells. Confocal microscopy was adopted to detect YFP and DAPI fluorescence in C666-1 cells treated or not treated with NA (40 μM). Statistical analyses of the percentage of cells contain four fields. All panels are of the same magnification ($\times 4000$) and each panel is representative of three experiments. Data shown are the mean + S.D. * $P < 0.05$. **(f)** The morphological changes of NA-treated cells were detected by TEM. All panels are of the same magnification ($\times 10000$) and each panel is representative of three experiments. **(g)** C666-1 cells were treated with NA (0–40 μM) for 8 h. Immunoblotting analysis was adopted to investigate the effect of NA on the expression level of LC3 and p62. β -Actin served as a loading control. **(h)** The cells were pretreated with Baf (1 μM) for 2 h and then treated with or without NA (40 μM) for an additional 6 h. The indicated proteins were detected by immunoblotting analysis. β -Actin served as a loading control

protein 1 (RIP1) is modified by cell death receptor-associated proteins, including cellular inhibitors of apoptosis (cIAPs) and cylindromatosis (CYLD), and forms a necrosome with RIP3 and eventually triggers necroptosis.^{13,14} Thus, considering the diverse forms of death in cancer cells, deciphering the underlying cell death mechanisms and relevant regulators in the exploration of new anticancer strategies is extremely important.

Energy metabolic reprogramming is another significant feature of most cancers. Multiple oncogenic signaling pathways and metabolic regulators are involved in the reprogramming process.¹⁵ A number of small-molecular compounds

that target metabolism-related pathways or regulators have been developed and shown activity in cancer cells.¹⁶ 3-phosphoinositide-dependent protein kinase 1 (PDK1), a serine/threonine kinase, can activate a group of protein kinases belonging to the AGC kinase family, including protein kinase A, protein kinase G and protein kinase C. PDK1 has pivotal roles in mediating energy metabolism, cell proliferation and migration.^{17,18} In response to various cellular stimulations, PDK1 can activate phosphoinositide-3 kinase (PI3-K) and then Akt.¹⁹ By upregulating multiple glycolytic genes such as the glucose transporters, hexokinases and lactate dehydrogenase, the PI3-K/Akt

signaling pathway increases glycolysis and couples intramitochondrial ATP synthesis to glucose metabolism.²⁰ In addition, by activating the anti-apoptotic effect of hexokinase 2 (HK2) in cancer cells, the PI3-K/Akt signaling pathway can inhibit early apoptotic events.²¹ On the basis of the important functions in tumor cells, PDK1 has been served as an effective therapeutic target for anticancer treatment.^{22,23}

In this study, we identified NA as a potent inhibitor of PDK1. By targeting PDK1, NA attenuated the PI3-K/Akt pathway and its downstream metabolic regulator, HK2, which eventually resulted in a striking energy crisis and cancer cell death. The activation of autophagy, energy crisis, presence of necrotic morphology, increase of RIP1/RIP3 colocalization and interaction, and reversed by Nec-1, which were all definitive standards of necroptosis,^{11,12} were clearly observed, indicating the induction of this non-apoptotic cell death mechanism. In addition, using a nasopharyngeal carcinoma (NPC) cell nude mouse model, we showed that NA decreased xenograft tumor growth and suppressed the PI3-K/Akt pathway *in vivo*. Taken together, our findings suggested that the PDK1-PI3-K/Akt signaling pathway might be involved in NA-induced apoptotic and necroptotic cell death by remodeling cellular energy metabolism, and therefore implied the potential of NA in anticancer treatment.

Results

NA selectively inhibits proliferation of cancer cells. The drimane-type sesquiterpenoid group of NA conjugates to resorcinol as a side chain and this isopentenyl-resorcine conjugation represents a brand-new type of carbon-backbone in natural compounds (Figure 1a; Supplementary Figure 1 and Tables 1 and 2). Thus, we hypothesized that compounds with this type of structure could have some as yet unidentified effects against cancer cells. To investigate the effect of NA in cancer cells, we treated six NPC cell lines (C666-1, HK1, SUNE1, HNE2-LMP1, CNE1-LMP1 and 5-8F), six breast cancer cell lines (ZR75-1, MX-1, T47D, MAD-MB-231, MDA-MB-453 and MCF-7), two colon cancer cell lines (HCT116 and SW620), one leukemia cell line (K562), one prostate cancer cell line (DU145), one lung adenocarcinoma epithelial cell line (A549), one melanoma cell line (A375) and three immortalized normal cell lines (human keratinocyte HaCaT, human nasopharynx epithelial NP69 and mouse fibroblast NIH/3T3) with NA. NA, even at 50 μ M, had no effect on the proliferation of normal immortalized HaCaT, NP69 or NIH/3T3 cells (Figure 1d; Supplementary Figure 2). However, in all the cancer cell lines tested, NA significantly inhibited proliferation in a dose-dependent manner, indicating the selectivity of NA toward cancer cells (Supplementary Figure 2). Moreover, among these cancer cell lines, C666-1 and HK1 NPC cells and ZR-75-1 breast cancer cells were most sensitive to NA with IC₅₀ values of about 10 μ M, 18 μ M and 7.5 μ M, respectively (Figure 1d, Supplementary Figure 2). In addition, by using propidium iodide (PI) staining and flow cytometry analysis, we found that NA induced a time- and dose-dependent death of cancer cells (Figures 1b and c). On the basis of

these data, we conclude that NA efficiently inhibits cancer cell growth.

NA induces apoptosis, autophagy and necroptosis of cancer cells.

To further investigate the mean by which NA kills cancer cells, annexin V-fluorescein isothiocyanate/PI (annexin V-FITC/PI) double staining and flow cytometry analysis were performed. NA treatment not only increased the percentage of annexin V-positive cells up to 78.2% but also induced the cleavage of caspases and PARP-1 in C666-1 cells, which indicated the activation of the apoptotic pathway (Figure 1c; Supplementary Figures 3a and b). Besides apoptosis, NA treatment also induced autophagy of C666-1, HK1 and CNE1 cells, as indicated by the upregulation of the protein level of endogenous LC3-II (Figure 1g; Supplementary Figure 3c). To further examine the effect of NA in the induction of autophagy, we transfected an LC3-fluorescence-expressing plasmid (that is, the LC3 gene fused to a yellow fluorescent protein, YFP-LC3) into C666-1 cells. Results (Figure 1e) indicated that compared with untreated cells where the YFP fluorescence was diffused in the cytoplasm, NA (40 μ M) treatment for 6 h led to punctuated aggregations of a strong YFP fluorescent signal in the cytosol. This aggregation of YFP fluorescent signal represented the existence of autophagy. The expression level of p62, which is degraded during autophagy, was gradually reduced in NA-treated cells (Figure 1g). To confirm that the changes in p62 were resulted from autophagy induction, a turnover assay for p62 to detect autophagic flux was conducted. In C666-1 cell lines, whereas either NA or the lysosome inhibitor Bafilomycin (Baf) alone induced a moderate increase of LC3-II, the cotreatment with both NA and Baf further elevated LC3-II level (Figure 1h). Consistently, the reduction of p62 induced by NA was effectively attenuated by Baf (Figure 1f). These data strongly substantiate that NA induces autophagy in cancer cells.

To examine the morphological changes of NA-treated cells, transmission electron microscopy (TEM) was adopted. Compared with untreated cells, NA treatment not only resulted in a rapid increase in the number of autophagic vacuoles but also induced extensive chromatin condensation in C666-1 cells (Figure 1f). However, these cells still retained an almost normal appearance of the nuclei with only a slight shrinkage. To further investigate NA-induced cell death, paclitaxel was used as a control to treat cells. Compared with cells treated with paclitaxel that exhibited classic apoptotic morphology such as condensed nuclei, cells treated with NA became irregular and swollen, which is almost always detected in necrosis (Figure 2a). Considering these morphological changes, we hypothesized that NA treatment might also cause necroptotic cell death, which is characterized by the activation of autophagy with a necrotic morphology. To test our hypothesis, we used Nec-1, a specific inhibitor of necroptosis, to preincubate with the NA-treated cells. Preincubation of cells with Nec-1 significantly prevented NA-induced death in C666-1 cells (Figure 2b), suggesting necroptosis as an important death pattern in NA-induced cell death. Because necroptosis is reportedly triggered by the interaction of RIP1 and RIP3 under stress, we analyzed the effect of NA on the interaction of these proteins in cancer cells.

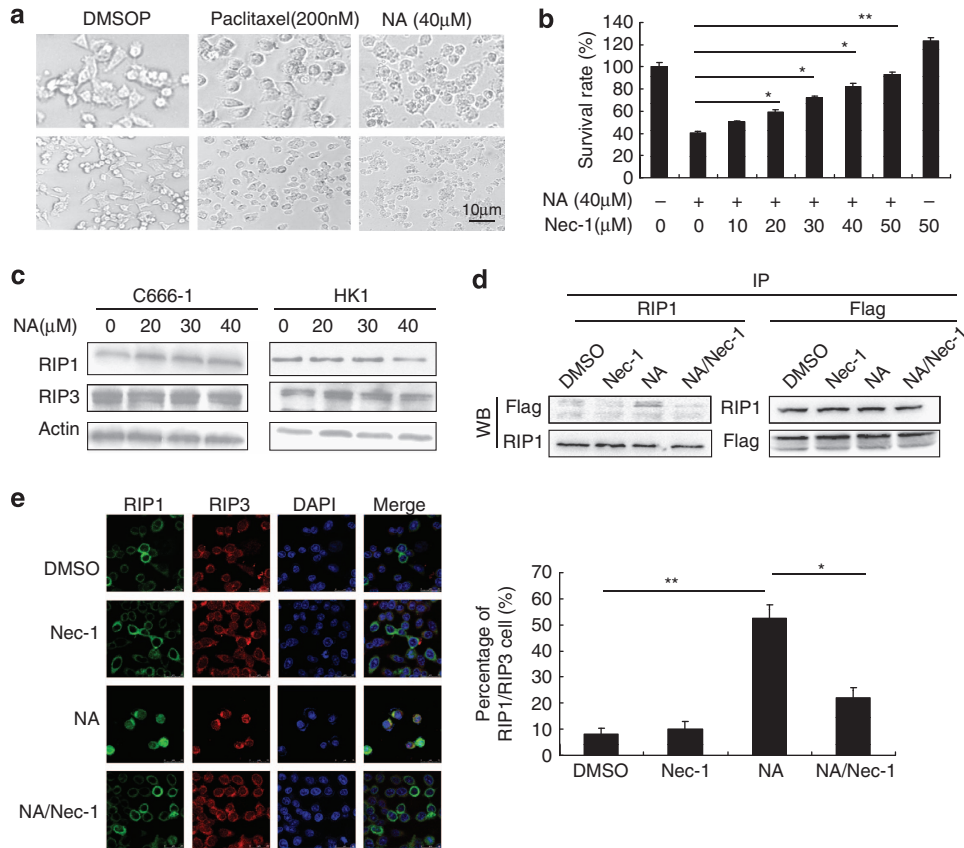


Figure 2 NA triggers necroptosis in cancer cells. (a) C666-1 cells were treated with NA (40 μ M), paclitaxel (200 nM) or DMSO. The effects on morphology of C666-1 cells were detected by optical microscopy. All panels are of the same magnification ($\times 100$ or $\times 40$) and each panel is representative of three experiments. (b) Nec-1(50 μ M) was preincubated with NA-treated cells. Cell viability was analyzed by the MTS assay. Data shown are the mean + S.D. of three experiments. * $P < 0.05$. ** $P < 0.001$. (c) Immunoblotting analysis was adopted to investigate the effect of NA on the expression level of RIP1 and RIP3. β -Actin served as a loading control. (d) A Flag-tagged RIP3 plasmid was transfected into C666-1 cells. A coimmunoprecipitation assay was used to analyze the effect of NA (40 μ M), Nec-1(50 μ M) or their combination on the interaction of RIP1 and RIP3. (e) The interaction of endogenous RIP1 and RIP3 was analyzed by an immunofluorescence confocal assay. Statistical analyses of the percentage of cells contain four fields. All panels are of the same magnification ($\times 1600$) and each panel is representative of three experiments. Data shown are the mean + S.D. * $P < 0.05$. ** $P < 0.001$

We transfected the Flag-tagged RIP3 plasmid into C666-1 cells. Results indicated that the protein expression level of RIP1 or RIP3 was not affected by NA treatment, and coimmunoprecipitation data revealed the binding of RIP1 and RIP3 in NA-treated cells (Figures 2c and d). The interaction and colocalization of endogenous RIP1 and RIP3 were also upregulated by NA as indicated in a confocal assay as increased fluorescence signaling (Figure 2e). Taken together, these findings suggested that NA induced apoptosis, autophagy and necroptosis in cancer cells.

NA targets PDK1 to suppress PI3-K/Akt signaling and its downstream target, HK2. To identify the potential cellular target of NA and clarify the underlying molecular mechanism in NA-induced cancer cell death, we first used the PHASE module of Schrödinger's molecular modeling software package to dock NA to potential protein targets. By this method, PDK1 was identified as a potential protein target of NA. More than three ligand-binding sites are located in the PDK1 kinase domain, including an ATP-binding pocket, a peptide substrate-binding site and a groove in the N-terminal lobe that binds to the C-terminal hydrophobic motif of the

kinase substrates. NA was able to dock into the ATP-binding pocket of PDK1 and form three hydrogen bonds with the backbone of PDK1 (Figure 3a). By using a kinase activity detection assay, NA was found to potently inhibit PDK1 kinase activity (Figure 3b). Immunoblotting analysis showed that, without affecting the phosphorylation level of PDK1, NA treatment suppressed the phosphorylation of Akt at Ser308, which is a direct substrate of PDK1 (Figure 3c). Moreover, NA inhibited the phosphorylation of Akt at Ser473 and Akt downstream molecules, including TSC2, mTOR and p70S6K1 in a dose-dependent manner (Figure 3d). When C666-1 cells were incubated with NA for a longer time, for 5 days, NA inhibited the phosphorylation of Akt and mTOR at much lower concentrations (Figure 3e). In addition, preincubation of C666-1 cells with NA could also suppress tumor necrosis factor- α (TNF α), epidermal growth factor (EGF), interleukin-6 (IL6) and fetal bovine serum (FBS)-induced activation of Akt (Figure 3f).

Because NA, by targeting PDK1, substantially suppressed the PI3-K/Akt signaling pathway, which is a central regulatory pathway in energy metabolic reprogramming in cancer cells, we examined several downstream metabolic regulators of this

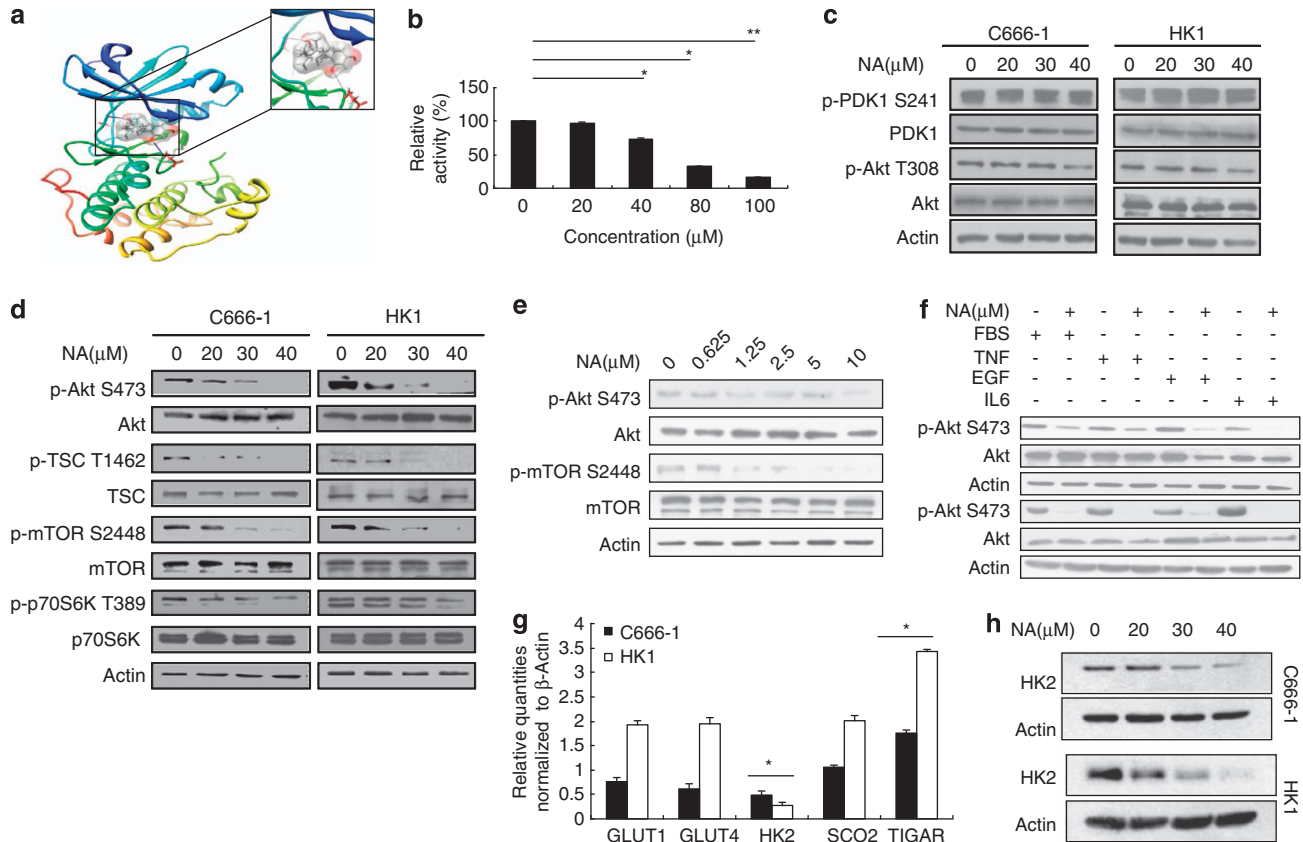


Figure 3 NA targets PDK1 to downregulate the PI3-K/Akt pathway and its downstream substrate HK2. (a) Computational modeling of the binding of NA and PDK1. The box indicates an enlarged view of the location of the hydrogen bonds. (b) The effect of NA on PDK1 kinase activity was analyzed by a human PDK1 kinase assay/inhibitor screening kit. Data shown are mean + S.D. of three experiments. * $P < 0.05$. ** $P < 0.001$. (c) The effect of NA (0–40 μM) on the expression level and the phosphorylation level of PDK1 and Akt was analyzed in C666-1 and HK1 cells by immunoblotting. β -Actin served as a loading control. (d) The effect of increasing doses of NA (0–40 μM) treatment for 8 h on the expression level and phosphorylation level of Akt and its downstream molecules, TSC2, mTOR, and p70S6K1 was analyzed by immunoblotting. β -Actin served as a loading control. (e) The effect of low doses of NA (0–10 μM) treatment for 5 days on the expression level and phosphorylation level of Akt and its downstream molecule, mTOR, was analyzed by immunoblotting. β -Actin served as a loading control. (f) The effect of NA on TNF α -, EGF-, IL6- or FBS-induced activation of Akt in C666-1 and HK1 cells was analyzed by immunoblotting. β -Actin served as a loading control. (g) The effect of NA (40 μM) on the downstream metabolic regulators (GLUT1, GLUT4 and HK2) of the Akt pathway was analyzed by quantitative real-time PCR in C666-1 and HK1 cells. Data shown are mean + S.D. of three experiments. (h) The effect of NA on the protein expression level of HK2 was analyzed by immunoblotting and α -tubulin, and β -Actin served as loading controls

pathway, including glucose transporter 1 (GLUT1), GLUT4 and HK2. Results indicated that the mRNA and protein level of HK2 was specifically downregulated by NA in C666-1 and HK1 cells (Figures 3g and h). In rapidly growing cancer cells, HK2 has been reported to be upregulated by PI3-K/Akt signaling in order to facilitate glycolysis.²⁴ On the basis of these findings, we suggest that NA might suppress HK2 by targeting the PDK1-PI3-K/Akt signaling pathway.

NA inhibits glucose consumption and ATP generation.

By targeting PDK1 and its downstream PI3-K/Akt pathway, NA inhibited the key energy metabolic enzyme HK2 in cancer cells. Thus, we proposed that NA treatment might affect cellular glucose metabolism. To test our idea, we treated C666-1 cells with NA for 4–6 h and then examined the glucose concentration in the medium and the cellular ATP generation. NA treatment not only significantly decreased the glucose concentration in the medium but also blocked ATP generation in a time-dependent manner (Figures 4a and b; Supplementary Figure 4). Moreover, even the necroptosis

inhibitor Nec-1 could rescue the viability of NA-treated cells; however, it was unable to reverse the ATP depletion in the time course tested (Figure 4c), indicating a cause-effect relationship between ATP depletion and necroptotic cell death. However, at longer incubation time point (48 h), Nec-1 could neither rescue cells from death nor reverse the ATP depletion (Supplementary Figure 5a). These mean that, by inhibiting necroptosis, Nec-1 could rescue cells from death at early stage of the energy short induced by NA, but cells dead after longer treatment of NA due to the persistent lack of energy supply.

To further confirm the role of Akt in HK2 expression and glucose metabolism, we transfected the myristoylated Akt (myr-Akt) plasmid into C666-1 cells. The presence of myr-Akt not only greatly elevated the mRNA and protein expression level of HK2 but also rescued the NA-inhibited Akt downstream pathway (Figures 4d and f). The cellular ATP level and cell viability were also measured after myr-Akt transfection. Results indicated that overexpression of Akt markedly elevated the cellular ATP level in NA-treated C666-1 cells

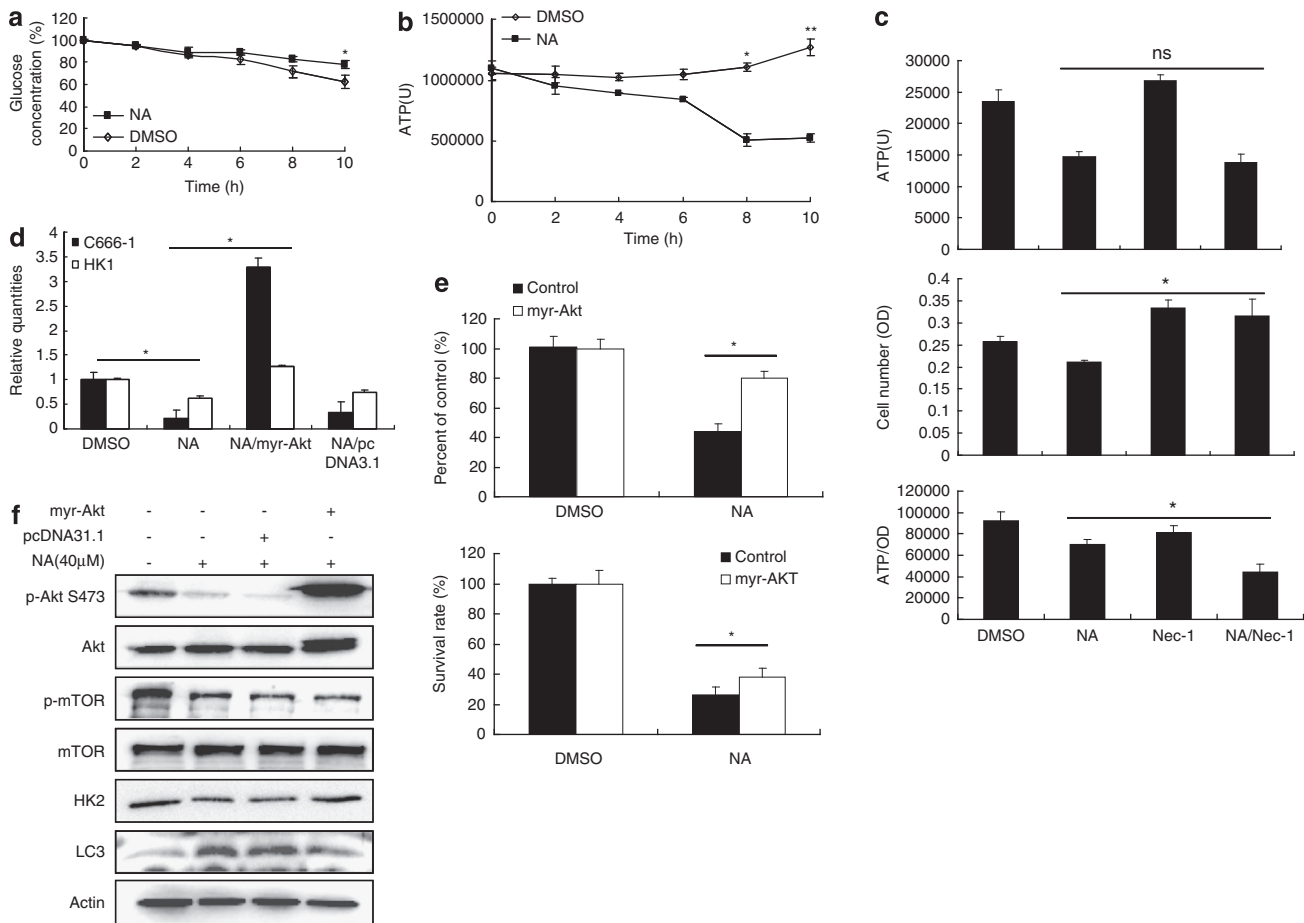


Figure 4 NA inhibits glucose consumption and ATP synthesis. (a and b) The effect of NA (40 μ M) treatment for 4–6 h on glucose consumption and ATP generation. Data are shown as mean \pm S.D. of three experiments. (c) The effect of NA on ATP synthesis in C666-1 cells was measured. Cells were incubated with NA(40 μ M), Nec-1 (40 μ M) or both for 24 h. ATP production and cell viability were determined and the average production of ATP per cell unit was calculated (ATP/OD). Data are shown as mean + S.D. of three experiments. * P < 0.05 ns, no significance. (d) The effect of Akt overexpression on NA-inhibited HK2 expression in C666-1 and HK1 cells was analyzed by quantitative real-time PCR. Data are shown as mean + S.D. of three experiments. * P < 0.05. (e) Cellular ATP level and cell viability were measured in Akt-overexpressing C666-1 cells. Data are shown as mean + S.D. of three experiments. * P < 0.05. (f) The expression level of Akt downstream molecules, mTOR, phosphorylated mTOR, HK2 and LC3 in NA-treated C666-1 cells was analyzed by immunoblotting. β -Actin served as a loading control

(Figure 4e). Also, overexpression of Akt could partially rescue the cell viability of NA-treated cells (Figure 4e). Moreover, Akt overexpression decreased LC3 expression and inhibited NA-induced autophagy (Figure 4f), implying that Akt inactivation and energy crisis are responsible for NA-induced autophagy.

NA-induced energy depletion results in cell death.

Under the stress of glucose metabolism dysfunction and energy depletion, cancer cells almost always undergo irreversible cell death. Here, apoptotic, autophagic and necroptotic cell death were induced by NA under energy depletion conditions. To investigate the role of necroptosis, apoptosis and autophagy in NA-induced cell death, specific inhibitors were used. Inhibition of autophagy by 3-methyladenine (3-MA) enhanced cell death in NA-treated cells, which suggested that autophagy might provide a survival force in NA-treated cells (Figure 5a; Supplementary Figure 3d). The apoptosis inhibitor benzyloxycarbonyl-Val-Ala-Asp(OMe)-fluoromethylketone (zVAD-fmk) and necroptosis inhibitor Nec-1 could rescue the viability of cells treated with NA

and 3-MA, which confirmed the role of apoptosis and necroptosis in NA-induced cell death (Figure 5a; Supplementary Figure 6). Under energy crisis, some cellular anti-death systems, such as the c-Jun NH (2)-terminal kinases (JNKs) pathway, are usually activated to support cell survival. Along with decreasing glucose consumption and ATP generation, JNKs were phosphorylated and activated by NA treatment (Figure 5b). Without affecting JNK activation and PARP cleavage, NAD⁺, a substrate for ATP synthesis, inhibited NA-induced LC3 expression and processing (Supplementary Figure 5b); it also effectively rescued cells from death (Supplementary Figure 5c). This to a certain degree confirmed that NA-induced ATP depletion was the cause of cell death. JNKs activation is reportedly able to induce autophagy when cells are starved, and a recent study demonstrated the capability of cancer cells to exploit autophagy as an energy source to support rapid cell proliferation.^{25,26} Here, the results showed that cotreatment with NA and SP600125 could further induced more cell death in HK1 and C666-1 cells (Figure 5c). On the basis of these

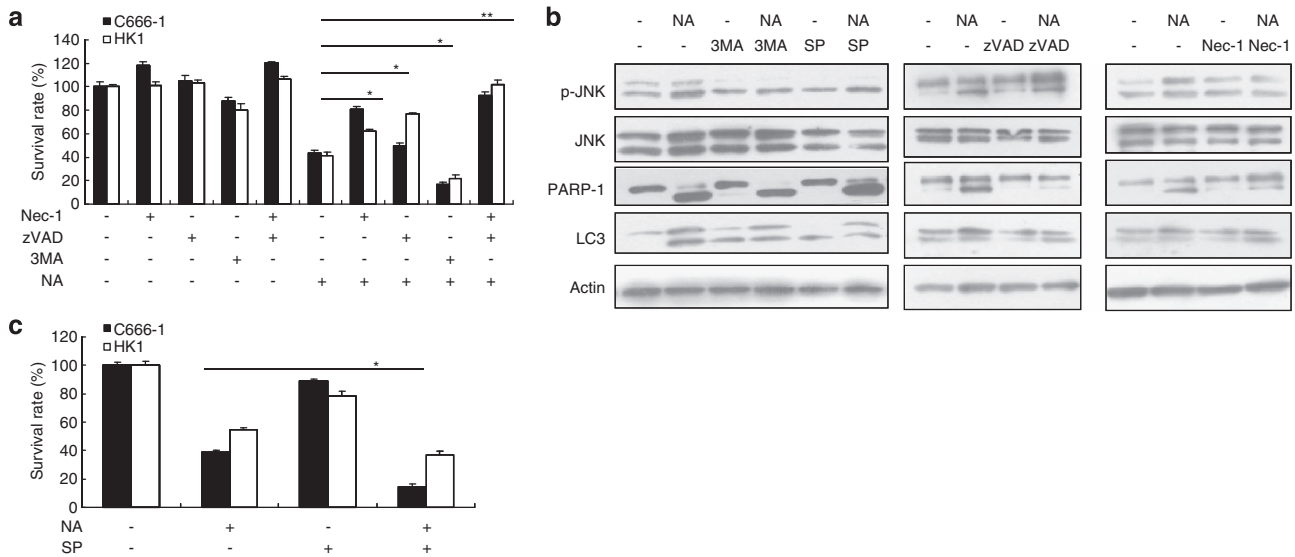


Figure 5 NA-induced dysfunction of glucose metabolism results in cell death. (a) Viability of C666-1 or HK1 cells treated with DMSO, NA(40 μ M), NA/Nec-1(40 μ M), NA/zVAD-fmk(20 μ M), NA/Nec-1/zVAD-fmk, NA/3-MA(5 mM), Nec-1, zVAD-fmk, Nec-1/zVAD-fmk or 3-MA was analyzed by MTS assay. Data are shown as mean + S.D. of three experiments. * $P < 0.05$. ** $P < 0.001$. (b) The effect of the autophagy inhibitor 3-MA(5 mM) or JNKs inhibitor SP600125(50 μ M), apoptosis inhibitor zVAD-fmk(20 μ M) and necroptosis inhibitor Nec-1 on the level of JNKs, phosphorylated JNKs, PARP-1 and LC3 was analyzed in C666-1 cells treated or not treated with NA. β -Actin served as a loading control. (c) The C666-1 cells were pretreated with SP600125 (50 μ M) for 1 h and then treated with or without NA (40 μ M) for an additional 24 h. The cell viability was analyzed by MTS. Data are shown as mean + S.D. of three experiments. * $P < 0.05$

findings, we suggest that NA-induced autophagy might provide a survival force in cancer cells, whereas apoptosis and necroptosis are responsible for NA-induced cell death.

Moreover, we found that the NA-mediated apoptosis, necroptosis and autophagy occurred independent of each other. Although both SP600125 and 3-MA significantly inhibited autophagy in cancer cells, neither SP600125 nor 3-MA could reverse the cleavage of PARP-1 (Figure 5b). This indicated that, even though NA-induced autophagy was related to the activation of JNKs, the NA-induced necroptosis and apoptosis occurred independently of JNKs activation (Figure 5b). Moreover, the apoptosis inhibitor zVAD-fmk suppressed PARP-1 cleavage but had little effect on NA-induced LC3 elevation or JNKs activation (Figure 5b). The necroptosis inhibitor Nec-1 was also unable to affect NA-induced apoptosis or autophagy in cancer cells (Figure 5b).

In vivo efficacy of NA in the NPC nude mouse model. To further evaluate the *in vivo* efficacy of NA, NPC C666-1 cells (5×10^6) were subcutaneously injected into the right anterior armpit of athymic nude mice. NA treatment (100 mg/kg/day) was initiated on the seventh day after transplantation when the tumors were established ($\sim 50 \text{ mm}^3$). On day 37 after transplantation, the average tumor volumes in the control group and NA-treated group increased to $1512 \pm 374 \text{ mm}^3$ and $627 \pm 260 \text{ mm}^3$, respectively (Figure 6a). The tumor volumes in the NA-treated group were significantly smaller than those in the vehicle-treated group. During the treatment period, the average body weight of mice in the NA-treated group was slightly lower than that of the control group, but none of the mice displayed evident signs of toxicity (Figure 6b). At the treatment end point, the mice were killed and tumors were removed and photographed (Figure 6c).

The average tumor weight of the control group and NA-treated group was $1.26 \pm 0.32 \text{ g}$ and $0.65 \pm 0.23 \text{ g}$, respectively (Figure 6d). Moreover, immunohistochemical examination of tumor sections from the model animals showed that phosphorylated mTOR, Akt and the expression of HK2 had been downregulated in the NA-treated group (Figure 6e). Consistent with the *in vitro* data, these data also indicated the efficacy of NA in inhibiting tumor growth by suppressing the Akt signaling pathway.

Discussion

More than 140 000 types of higher fungi exist in the world, but only 10% of them have been identified. More efforts are needed to investigate and explore the potential of fungi as an anticancer treatment.^{27,28} NA, a novel small-molecular compound that was isolated from the fungus *Albatrellus yasuda* of the family *Polyporaceae*. In this study, NA showed potency in inhibiting the growth of a broad spectrum of tumor cell lines, especially for NPC and breast cancer cells. NA not only induced apoptotic and necroptotic cell death but also caused autophagy. By using computer-based target screening, PDK1 was identified as a direct target for NA. PDK1 is a vital regulator in multiple extracellular stimuli-mediated pathways and has a role in Akt activation.^{18,29} The PDK1 signaling pathway is almost always hyperactivated in human cancer cells, which makes it an ideal target for anticancer therapy.³⁰ In recent years, many small-molecular inhibitors of PDK1 have been developed.^{31,32} Our data demonstrated that by targeting to PDK1 and blocking its kinase activity, NA potently inhibited the PI3-K/Akt pathway and its downstream metabolic regulator HK2, which eventually resulted in ATP depletion and dysfunction of glucose metabolism. The PI3-K/Akt pathway is

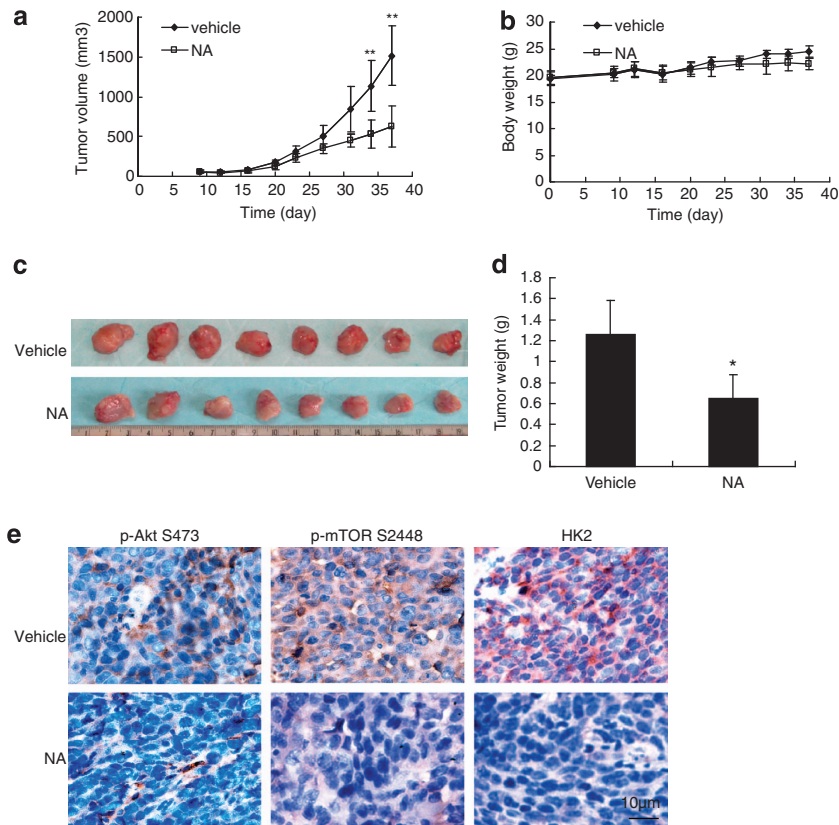


Figure 6 The *in vivo* efficacy of NA in an NPC nude mouse model. (a) C666-1 cells were subcutaneously injected into the right flank of mice and tumor volumes in the control group and NA-treated group were measured every day. On day 37 after transplantation, when the average tumor volumes of control tumors exceeded 1 cm³, the mice were killed. Data are shown as mean \pm S.D. of eight mice. (b) During the treatment period, the effect of NA on the average body weight of mice was measured every day. Data are shown as mean \pm S.D. of eight mice. (c) At the treatment end point, mice were killed and tumors were removed and photographed. (d) The tumor weight of mice from control group and NA-treated group was measured. Data are shown as mean \pm S.D. of eight mice. (e) Immunohistochemical examinations of phosphorylated mTOR, Akt and the expression of HK2 in tumor sections from control mice and NA-treated mice. All panels are of the same magnification ($\times 400$)

an important signal transduction system for cellular energy metabolism, and a variety of small molecules that block PI3-K/Akt signaling have been explored for their ability to reverse the malignant phenotypes in cancer cells.³³ As a downstream molecule in the Akt pathway, HK2 is not only able to regulate glucose metabolism but also exhibits an anti-cell death effect by blocking the voltage-dependent anion channel (VDAC).^{20,34} On the basis of these findings, we suggest that NA induced energy depletion and triggered cell death through the inhibition of the PI3-K/Akt signaling pathway.

Cancer cells almost always have deficiencies in the induction of apoptosis resulting in anticancer drug resistance and induction of alternative, non-apoptotic cell death may provide therapeutic benefits in cancer cells, especially in apoptosis-defective cancer cells.³⁵ Simultaneously, the activation of multiple cell death pathways may help to overcome chemotherapy resistance results from single death mode killing. Obatoclax, a pan-anti-apoptotic BCL-2 family small-molecule inhibitor, induced cell death in a unique mixed form of death involving apoptosis, necroptosis and autophagy.³⁶ It may help to overcome chemotherapy resistance in infant ALL. Here, we found that apoptosis and necroptosis were responsible for the death-inducing efficacy of NA, whereas necroptosis might be more important in NA-induced cell death in NPC cells. Because autophagic vesicles are commonly

observed in necroptotic cells, some researchers propose that autophagy is a major mechanism for necroptosis.^{11,12} In mouse L929 fibroblasts, attenuation of autophagy by the inhibitor 3-MA or knockdown of autophagy-related genes has been shown to block necroptosis.³⁷ But in Jurkat lymphoma cells, the inhibition of autophagy is unable to suppress necroptosis.¹¹ The role of autophagy in cell viability is reported to be dependent on context but remains controversial.²⁶ Several investigators have demonstrated that when cells are exposed to various stresses, JNKs are activated to induce autophagy.^{38–40} Some studies suggest that cancer cells can exploit autophagy as an energy source to support rapid cell growth,^{25,26} which implies that autophagy acts as a survival force to protect cells from energy depletion.

In this study, we found that in response to the NA-induced metabolic stress, autophagy was activated by the JNKs pathway. This NA-induced autophagy occurred independent from apoptosis and also was not relevant for the execution of necroptosis in cancer cells. Inhibition of autophagy by a JNKs inhibitor or 3-MA could markedly facilitate NA-induced cell death, which suggested that autophagy provided a survival advantage for these energy-depleted cells. As is well known, blood vessels are absent at the center of a solid tumor mass and cancer cells usually lack a sufficient supply of energy materials. Thus, the survival force provided by autophagy

might be more important to cancer cells under this condition of energy shortage.^{26,41} However, if the energy shortage is aggravated by suppressing the energy-generation glycolytic pathway in these cells, autophagy might be unable to rescue cells from irreversible cell death. Therefore, in this study, autophagy provided a survival advantage but could not reverse NA-induced energy depletion and irreversible cell death.

This study is the first to demonstrate the antitumor effect of the newly identified natural compound NA in cancer cells and in a xenograft mouse model. The ability of NA to target PDK1 and its downstream PI3-K/Akt pathway revealed an interfering function of NA in an oncogenic signaling network, and especially in energy metabolism and cell death cascade signaling pathways in cancer cells (see Figure 7). HK2, a regulator involved not only in the Warburg effect but also in the anti-apoptosis process, were inhibited in NA-treated cells and thus resulted in an energy crisis, which eventually led to apoptotic and necroptotic cell death. Even though autophagy could provide a survival advantage under NA-mediated energy depletion stress, it was still unable to reverse NA-induced cell death. With these discoveries, we suggest that by targeting the PDK1-PI3-K/Akt-energy metabolic pathway, NA might be a leading compound for cancer therapy and chemoprevention.

Materials and Methods

Cell lines and culture. The following cell lines were used: NPCs (C666-1, CNE1, HK-1, HNE2-LMP1, CNE1-LMP1, SUNE1 and 5-8F), chronic myelogenous leukemia cells (K562), human lung adenocarcinoma epithelial cells (A549), human amelanotic melanoma cells (A375), human breast cancer cells (MX-1, MCF-7, T47D, ZR-75-1, MDA-MB-231 and MDA-MB-453), human colon carcinoma cells (HCT116 and SW620), human keratinocyte cells (HaCaT), mouse embryonic fibroblasts cells (NIH/3T3) and human immortalized nasopharyngeal epithelial cells (NP69).

All cells except NP69 were cultured in RPMI-1640 medium (Gibco/BRL, Grand Island, NY, USA) containing 10% FBS, 100 units/ml penicillin and 100 mg/ml

streptomycin. The NP69 immortalized nasopharyngeal epithelial cells were grown in a 1:1 mixture of Defined Keratinocyte-SFM (Gibco) and EpiLife™ medium with growth supplements (Cascade Biologics, Portland, OR, USA). All cells were cultured in a humidified atmosphere with 5% CO₂ at 37 °C.

Reagents. NA was isolated and identified from the mushroom *Albatrellus confluens*. Nec-1, 3-MA, zVAD-fmk and paclitaxel, SP600125, DMSO, EGF, IL6 and TNF α were purchased from Sigma-Aldrich (St. Louis, MO, USA). FBS and Lipofectamin were purchased from Invitrogen (Carlsbad, CA, USA).

Antibodies against caspase 3, caspase 8, caspase 9, PARP-1, HK2, SAPK/JNKs and SAPK/JNKs (Thr183/Tyr185), Akt, Akt (Ser473), S6K1, S6K1 (Thr389), mTOR and mTOR (Ser2448) were purchased from Cell Signaling (Beverly, MA, USA). Antibodies against β -actin, α -tubulin, donkey anti-goat IgG-HRP, goat anti-rabbit IgG-HRP and goat anti-mouse IgG-HRP were purchased from Santa Cruz Biotechnology (Santa Cruz, CA, USA). The antibody against LC3 was purchased from Novus Biological (Littleton, CO, USA).

Plasmids. The pcDNA3.1-myr-AKT and pcDNA3.1-YFP-LC3 plasmids were kindly provided by Dr. Xiao-Feng Zhu (Sun Yat-Sen University, Guangzhou, China). The empty construct pcDNA3.1 was transfected as a control. The Flag-RIP3 plasmid was kindly provided by Xiaodong Wang (National Institute of Biological Sciences, Beijing, China).

Cell viability and flow cytometry assay. Cell viability was measured using a CellTiter-Glo Luminescent Cell Viability Assay kit (MTS) purchased from Promega Corp. (Madison, WI, USA) and used according to the manufacturer's protocol.

For flow cytometry assay of apoptosis and cell cycle, C666-1 and HK-1 cells were incubated with 40 μ M NA for 24 h. Cells (1×10^6 cells/ml) were resuspended in binding buffer and 0.5 ml of the suspension were transferred to a microfuge tube. After adding 5 μ l Annexin V-FITC and 5 μ l PI, cells were incubated at room temperature for 15 min in the dark. Apoptosis was analyzed by flow cytometry (Beckman Coulter, Fullerton, CA, USA).

Measurement of ATP. ATP levels were measured using an assay kit from Perkin Elmer (Boston, MA, USA) as described in the manufacturer's protocol.

Detection of glucose in the culture medium. Cells were seeded in six-well plate. After 24 h, culture medium was replaced with fresh medium with or without 40 μ M NA and cells were incubated at 37 °C. At the time-point indicated, a 500 μ l sample of culture medium was collected and assayed for glucose in an automatic biochemistry analyzer (Hitachi, 7170A, Tokyo, Japan).

Western blotting analysis. Cell disruption and immunoblotting were performed as described previously.⁴² After harvesting and disrupting the cells, protein lysates were electrophoresed in SDS polyacrylamide gels and transferred to nitrocellulose membranes. Specific protein bands were visualized by an enhanced Western lightening plus-ECL kit (Pierce, Rockford, IL, USA). β -Actin and α -tubulin were used as loading controls.

Transmission electron microscopy. Cells were fixed with 2.5% glutaraldehyde for 24 h. Post fixation was performed in 2% osmium tetroxide for 2 h followed by standard procedures for dehydration. Cells were embedded in Epon, and sections were prepared by ultramicrotome, collected on copper grids, stained with uranyl and lead citrate and observed with electron microscopy (Hitachi, H-7500, Tokyo, Japan).

Confocal microscopy. After transfection with YFP-LC3 or empty vector, cells were grown in chamber slides (Thermo, Rochester, NY, USA) for 24 h and then treated with 40 μ M NA for 8 h. After cells were fixed with 4% paraformaldehyde in PBS for 30 min at room temperature, the slides were mounted in anti-fade reagent with DAPI (Invitrogen, Eugene, OR, USA) and observed with a laser-scanning confocal microscope (Olympus, Tokyo, Japan) using the FV10-ASW Detection System (Applied Biosystems, Foster City, CA, USA).

PDK1 kinase assay. PDK1 kinase was measured using a kinase assay/inhibitor screening kit from CycLex Co. Ltd. (Ina, Nagano, Japan) as described in the manufacturer's protocol.

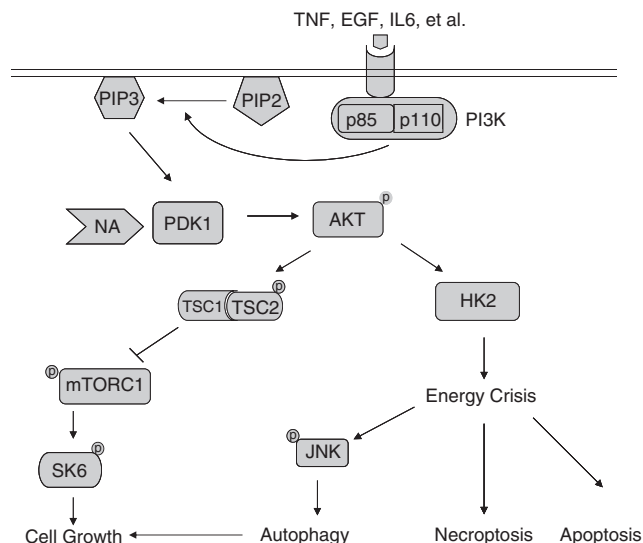


Figure 7 A schematic illustrating a model of NA anticancer activity is proposed. NA is suggested to target PDK1 and suppress its downstream Akt, mTOR and HK2 protein targets, resulting in a cellular energy crisis. Even though autophagy, which was induced by stress-activated JNKs, could provide a survival advantage in NA-treated cells, it was unable to prevent apoptotic and necroptotic cell death in response to this energy depletion

Real-time PCR. Cells were treated with NA (40 μ M) for 8 h followed by RNA extraction. Total RNA was reverse transcribed into cDNA using SuperScript II Reverse Transcriptase (Invitrogen) according to the manufacturer's recommendations. To measure mRNA expression, quantitative real-time PCR was conducted using the ABI PRISM 7500 Sequence Detection System (Applied Biosystems). The primers were synthesized by Sangon Biotech (Shanghai, China) and included the following: *GLUT1*, 5'-GATTGGCTCCTTCTCTGTGG-3' and 5'-TCAAAGGACTTGCCAGTTT-3', *GLUT4*, 5'-CCCCTCAGAAGGTGATTGAA-3' and 5'-CTTTCC TTCCAAGCCACTG-3', *HK2*, 5'-CAAAGTGACAGTGGGTGTGG-3' and 5'-GCCA GGTCTTCACTGTCTC-3', *SCO2*, 5'-GAGGCTTGAGCTGAGAGAGC-3' and 5'-CTCGTGTGGTCCACTGAC-3', *TIGAR*, 5'-AGGTAGCCCGCAGTGCAGG G-3' and 5'-CCGGCGGTGTAACACAGGG-3, β -actin, 5'-TTCCAGCCTTCTT CCTGGG-3' and 5'-TTGCGCTCAGGAGGACAAT-3'.

Xenograft NPC mouse model and immunohistochemistry. The animal studies were conducted according to the standards established by the Guidelines for the Care and Use of Laboratory Animals of Central South University. All the animals used in this study (4- to 6-week-old, male BALB/c nu/nu nude mice) were purchased from the Animal Center of Central South University and maintained in a laminar airflow cabinet under specific pathogen-free conditions in the Laboratory for Experiments, Central South University. C666-1 cells were subcutaneously injected into the right anterior armpit of mice (5×10^6 cells per mouse). After the tumors were established ($\sim 50 \text{ mm}^3$), mice were randomly divided into two groups of eight each and were treated or not treated with NA (100 mg/kg/d). The body weight of each mouse was recorded, and tumor volume was determined by Vernier caliper, following the formula of $(a \times b^2)/2$, where a is the longest diameter of tumor and b is the shortest diameter. After 30 d of treatment, the mice were killed and solid tumors were removed and photographed and then fixed with 10% formaldehyde and embedded in paraffin. Tumor sections (5 μ m) were used for immunohistochemical analysis using the appropriate antibodies. Images were taken with the Olympus photomicroscope (Olympus). Immunohistochemical results were diagnosis by two experienced pathologists.

Statistical analysis. Data are presented as mean \pm S.D. and statistical comparisons between the treated and untreated groups were performed using one-way ANOVA followed by Dunnett's test. *P*-values of ≤ 0.05 were considered statistically significant.

Conflict of Interest

The authors declare no conflict of interest.

Acknowledgements. We thank Professor Qiao Wu (School of Life Science, Xiamen University, China), Prof. Wenbin Zeng (School of medicine, Central South University, China) and Prof. Lun-Quan Sun (Xiangya Hospital, Central South University, China) for their helpful discussions and kind advice. We also thank Dr. Xiao-Dong Wang (National Institute of Biological Sciences, China) for providing the Flag-RIP3 plasmid. We thank Dr. Xiao-Feng Zhu (The State Key Laboratory of Oncology in South China, Sun Yat-Sen University, China) for providing the pcNDA3.1-myr-Akt and pcNDA3.1-YFP-LC3 plasmids. This work was supported by the National Basic Research Program of China (2009CB522300); the National Nature Science Foundation of China (90813028 and 30830113); and Hunan Provincial Innovation Foundation for Postgraduate.

- Lindequist U, Niedermeyer TH, Julich WD. The pharmacological potential of mushrooms. *Evid Based Complement Alternat Med* 2005; **2**: 285–299.
- Purvis A, Hector A. Getting the measure of biodiversity. *Nature* 2000; **405**: 212–219.
- Luo XJ, Li LL, Deng QP, Yu XF, Yang LF, Luo FJ et al. Grifolin, a potent antitumor natural product upregulates death-associated protein kinase 1 DAPK1 via p53 in nasopharyngeal carcinoma cells. *Eur J Cancer* 2011; **47**: 316–325.
- Liu Q, Shu X, Wang L, Sun A, Liu J, Cao X. Albaconol, a plant-derived small molecule, inhibits macrophage function by suppressing NF-kappaB activation and enhancing SOCS1 expression. *Cell Mol Immunol* 2008; **5**: 271–278.
- Hellwig V, Nopper R, Mauler F, Freitag J, Ji-Kai L, Zhi-Hui D et al. Activities of prenylphenol derivatives from fruitbodies of *Albatrellus* spp. on the human and rat vanilloid receptor 1 (VR1) and characterisation of the novel natural product, confluentin. *Archiv der Pharmazie* 2003; **336**: 119–126.

- Hanahan D, Weinberg RA. Hallmarks of cancer: the next generation. *Cell* 2011; **144**: 646–674.
- Kroemer G, Galluzzi L, Vandenabeele P, Abrams J, Alnemri ES, Baehrecke EH et al. Classification of cell death: recommendations of the Nomenclature Committee on Cell Death 2009. *Cell Death Differ* 2009; **16**: 3–11.
- Galluzzi L, Vitale I, Abrams JM, Alnemri ES, Baehrecke EH, Blagosklonny MV et al. Molecular definitions of cell death subroutines: recommendations of the Nomenclature Committee on Cell Death 2012. *Cell Death Differ* 2012; **19**: 107–120.
- Kabeya Y, Mizushima N, Ueno T, Yamamoto A, Kirisako T, Noda T et al. LC3, a mammalian homologue of yeast Ap8p, is localized in autophagosome membranes after processing. *EMBO J* 2000; **19**: 5720–5728.
- Tanida I, Ueno T, Kominami E. LC3 conjugation system in mammalian autophagy. *Int J Biochem Cell Biol* 2004; **36**: 2503–2518.
- Degterev A, Huang Z, Boyce M, Li Y, Jagtap P, Mizushima N et al. Chemical inhibitor of nonapoptotic cell death with therapeutic potential for ischemic brain injury. *Nat Chem Biol* 2005; **1**: 112–119.
- Yuan J, Kroemer G. Alternative cell death mechanisms in development and beyond. *Genes Dev* 2010; **24**: 2592–2602.
- Han J, Zhong CQ, Zhang DW. Programmed necrosis: backup to and competitor with apoptosis in the immune system. *Nature Immunol* 2011; **12**: 1143–1149.
- Vandenabeele P, Galluzzi L, Vanden Berghe T, Kroemer G. Molecular mechanisms of necroptosis: an ordered cellular explosion. *Nat Rev Mol Cell Biol* 2010; **11**: 700–714.
- Jones RG, Thompson CB. Tumor suppressors and cell metabolism: a recipe for cancer growth. *Genes Dev* 2009; **23**: 537–548.
- Tennant DA, Duran RV, Gottlieb E. Targeting metabolic transformation for cancer therapy. *Nature Rev Cancer* 2010; **10**: 267–277.
- Alessi DR, Deak M, Casamayor A, Caudwell FB, Morrice N, Norman DG et al. 3-Phosphoinositide-dependent protein kinase-1 (PDK1): structural and functional homology with the *Drosophila* DSTPK61 kinase. *Curr Biol* 1997; **7**: 776–789.
- Mora A, Komander D, van Aalten DM, Alessi DR. PDK1 the master regulator of AGC kinase signal transduction. *Semin Cell Dev Biol* 2004; **15**: 161–170.
- Toker A, Newton AC. Cellular signaling: pivoting around PDK-1. *Cell* 2000; **103**: 185–188.
- Wolf A, Agnihotri S, Micallef J, Mukherjee J, Sabha N, Cairns R et al. Hexokinase 2 is a key mediator of aerobic glycolysis and promotes tumor growth in human glioblastoma multiforme. *J Exp Med* 2011; **208**: 313–326.
- Robey RB, Hay N. Mitochondrial hexokinases, novel mediators of the antiapoptotic effects of growth factors and Akt. *Oncogene* 2006; **25**: 4683–4696.
- Raimondi C, Falasca M. Targeting PDK1 in cancer. *Curr Med Chem* 2011; **18**: 2763–2769.
- Bhola NE, Freilino ML, Joyce SC, Sen M, Thomas SM, Sahu A et al. Antitumor mechanisms of targeting the PDK1 pathway in head and neck cancer. *Mol Cancer Ther* 2012; **11**: 1236–1246.
- Mathupala SP, Ko YH, Pedersen PL. Hexokinase II: cancer's double-edged sword acting as both facilitator and gatekeeper of malignancy when bound to mitochondria. *Oncogene* 2006; **25**: 4777–4786.
- Gozuacik D, Kimchi A. Autophagy as a cell death and tumor suppressor mechanism. *Oncogene* 2004; **23**: 2891–2906.
- Kondo Y, Kanzawa T, Sawaya R, Kondo S. The role of autophagy in cancer development and response to therapy. *Nat Rev Cancer* 2005; **5**: 726–734.
- Myers N, Mittermeier RA, Mittermeier CG, da Fonseca GA, Kent J. Biodiversity hotspots for conservation priorities. *Nature* 2000; **403**: 853–858.
- Joppa LN, Roberts DL, Myers N, Pimm SL. Biodiversity hotspots house most undiscovered plant species. *Proc Natl Acad Sci USA* 2011; **108**: 13171–13176.
- Alessi DR, James SR, Downes CP, Holmes AB, Gaffney PR, Reese CB et al. Characterization of a 3-phosphoinositide-dependent protein kinase which phosphorylates and activates protein kinase B alpha. *Curr Biol* 1997; **7**: 261–269.
- Osaki M, Oshimura M, Ito H. PI3K-Akt pathway: its functions and alterations in human cancer. *Apoptosis* 2004; **9**: 667–676.
- Peifer C, Alessi DR. Small-molecule inhibitors of PDK1. *Chem Med Chem* 2008; **3**: 1810–1838.
- Bobkova EV, Weber MJ, Xu Z, Zhang YL, Jung J, Blume-Jensen P et al. Discovery of PDK1 kinase inhibitors with a novel mechanism of action by ultrahigh throughput screening. *J Biol Chem* 2010; **285**: 18838–18846.
- Yuan TL, Cantley LC. PI3K pathway alterations in cancer: variations on a theme. *Oncogene* 2008; **27**: 5497–5510.
- Jiang S, Zhang LF, Zhang HW, Hu S, Lu MH, Liang S et al. A novel miR-155/miR-143 cascade controls glycolysis by regulating hexokinase 2 in breast cancer cells. *EMBO J* 2012; **31**: 1985–1998.
- Mathiasen IS, Jaattela M. Triggering caspase-independent cell death to combat cancer. *Trends Mol Med* 2002; **8**: 212–220.
- Urishak KA, Edwards AY, Wang LS, Hudome A, Robinson BW, Barrett JS et al. Potent obatoclax cytotoxicity and activation of triple death mode killing across infant acute lymphoblastic leukemia. *Blood* 2013; **121**: 2689–2703.

37. Yu L, Alva A, Su H, Dutt P, Freundt E, Welsh S *et al*. Regulation of an ATG7-beclin 1 program of autophagic cell death by caspase-8. *Science* 2004; **304**: 1500–1502.
38. Davis RJ. Signal transduction by the JNK group of MAP kinases. *Cell* 2000; **103**: 239–252.
39. Wei Y, Pattingre S, Sinha S, Bassik M, Levine B. JNK1-mediated phosphorylation of Bcl-2 regulates starvation-induced autophagy. *Mol Cell* 2008; **30**: 678–688.
40. Sun T, Li D, Wang L, Xia L, Ma J, Guan Z *et al*. c-Jun NH2-terminal kinase activation is essential for up-regulation of LC3 during ceramide-induced autophagy in human nasopharyngeal carcinoma cells. *J Transl Med* 2011; **9**: 161.
41. Xu ZX, Liang J, Haridas V, Gaikwad A, Connolly FP, Mills GB *et al*. A plant triterpenoid, avicin D, induces autophagy by activation of AMP-activated protein kinase. *Cell Death Diff* 2007; **14**: 1948–1957.
42. Burnette WN. 'Western blotting': electrophoretic transfer of proteins from sodium dodecyl sulfate–polyacrylamide gels to unmodified nitrocellulose and radiographic detection with antibody and radioiodinated protein A. *Anal Biochem* 1981; **112**: 195–203.



Cell Death and Disease is an open-access journal published by Nature Publishing Group. This work is licensed under a Creative Commons Attribution-NonCommercial-ShareAlike 3.0 Unported License. To view a copy of this license, visit <http://creativecommons.org/licenses/by-nc-sa/3.0/>

Supplementary Information accompanies this paper on Cell Death and Disease website (<http://www.nature.com/cddis>)